

Haptic Object Recognition using Passive Joints and Haptic Key Features

Nicolas Gorges, Stefan Escaida Navarro, Dirk Göger, and Heinz Wörn
Institute for Process Control and Robotics
Karlsruhe Institute of Technology
Karlsruhe, Germany
e-mail:{gorges, escaida, goeger, woern}@ira.uka.de

Abstract—This paper presents a novel approach for haptic object recognition with an anthropomorphic robot hand. Firstly, passive degrees of freedom are introduced to the tactile sensor system of the robot hand. This allows the planar tactile sensor patches to optimally adjust themselves to the object’s surface and to acquire additional sensor information for shape reconstruction. Secondly, this paper presents an approach to classify an object directly from the haptic sensor data acquired by a palpation sequence with the robot hand – without building a 3d-model of the object. Therefore, a finite set of essential finger positions and tactile contact patterns are identified which can be used to describe a single palpation step. A palpation sequence can then be merged into a simple statistical description of the object and finally be classified. The proposed approach for haptic object recognition and the new tactile sensor system are evaluated with an anthropomorphic robot hand.

I. INTRODUCTION

Handling unknown objects with a robotic hand has been a subject of research the recent years and has become even more important. An active palpation sequence with direct interaction with the object allows perceiving object features like shape, texture and weight which are essential for handling an object. In this context there exist two major problems: the haptic perception of the robot hand and the creation of an object model through haptic perception.

The haptic perception of a robotic hand usually includes *tactile* sensing for surface sensibility and *kinesthetic* sensor data like the finger positions for depth sensibility. A tactile sensor matrix allows taking small imprints of the object which can be used to recognize simple surface structures [1]. A tactile sensor matrix can be arranged on a plane or on a curved surface. Planar tactile sensor patches have the benefit that they can take a full imprint of an object’s surface resulting in a tactile image. As a drawback, the object tends to adapt its position and orientation according to the planar surface of the sensor before a contact can be detected. A curved tactile sensor patch [2] has the benefit that it can measure contacts from several directions. But the tactile images of these sensor matrices are limited to point contacts and do not take a full imprint of the surface structure.

In this paper, we introduce a tactile sensor system which merges the benefits of both sensor types: firstly, it consists of planar sensor patches taking tactile imprints of the object surface and secondly, a sensor patch is mounted on a mini-joystick gaining two passive degrees of freedom. These passive joints make the tactile sensor adapt itself to the object

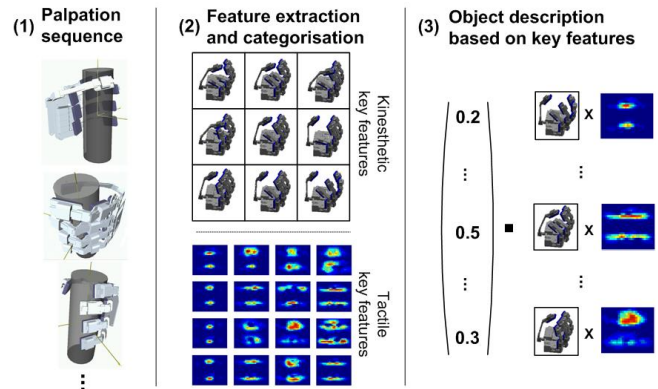


Fig. 1. From a palpation sequence to an object description using haptic key features: (1) An object is successively enfolded. (2) Key haptic features including joint angles and tactile patterns are extracted by clustering from example palpations. (3) Each single palpation is mapped on these key haptic features. Then, each entry of the object vector tells the percentage of how often the according haptic feature occurred during the palpation sequence.

surface in case of contact and provides essential information for shape reconstruction.

Concerning the generation of an object model through haptic perception, previous work [3] concentrates on the collection of a point cloud from haptic exploration data. As an additional processing step, the point cloud can be approximated by a volumetric object model and the object can be classified [4], [5]. The problem with these approaches is that the fusion into a single object model becomes inaccurate as soon as the object moves – which is likely to happen having a direct interaction with the object. Therefore, these approaches assume that the object is fixed and not moveable. Furthermore, the whole kinematic chain from the tactile sensors to the robot coordinate system must be known.

Alternatively, recent work tries to build an object model directly from haptic sensor data without building a 3d-model. In [6], objects are explored with a single tactile sensor matrix mounted on a robotic arm. The objects are classified directly from a tactile image sequence perceived through a palpation sequence. In [7], [8], objects were categorized according to their shape from a single grasp. The system was able to generalize 6 novel objects. In [9] was shown that through repeated grasping the object converges into a stable grasping state and the variance of the sensor data for perceiving an object of the same class is reduced. The sensor data of a

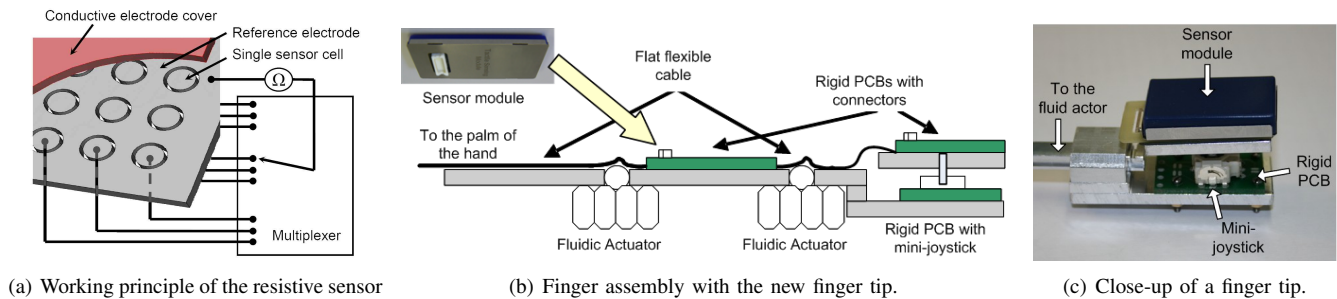


Fig. 2. Sensor working principle and layout.

converged grasp qualifies for making a statement about the shape and the identity of an object. Recent work [10] learns a vocabulary from tactile observations to classify an object from several grasp actions with a two-finger gripper.

Our work addresses the scenario of an anthropomorphic robot hand successively unfolding an object. We want to perceive the partial shapes of an object and to explicitly use the variance of the haptic sensor data. As depicted in Fig. 1, the idea is to find a limited amount of kinesthetic key features (finger configurations) combined with tactile key contact patterns which allow describing the perceived haptic data and therefore the partial geometry of an object at its best. We call this combination of tactile and kinesthetic key features *haptic key features*. The haptic key features are automatically identified using methods from machine learning. Each single palpation of a palpation sequence can then be mapped on these categories. The proposed object descriptor is based on the histogram of the key features and includes the percentages of how often certain haptic key features occurred during a palpation sequence. There will be no need for a kinematic model of the hand as the angles of the fingers are directly used without further processing. The object is explicitly allowed to be moved as there is no need for a reference coordinate system. The evaluation of this approach and of the proposed tactile sensor system will be done with two versions of the robot hand: the first one has only rigid tactile sensor patches without passive joints and the second one is equipped at the finger tips with the proposed tactile sensor modules having two additional rotatory degrees of freedom.

After this introduction, the robot hand and the tactile sensor system are explained in section II. The workflow of the object recognition approach is organized in four chapters: the feature extraction of the sensor data is described in section III followed by section IV which shows the categorisation of these features. Section V explains how to create an object descriptor based on the determined categories and section V shows the object classification based on these object descriptors. The results of our approach are presented in section VI followed by the conclusions in section VII.

II. TACTILE SENSOR SYSTEM

A. Sensor design and working principle

We consider two versions of a tactile sensor system: on the one hand, a rigid tactile sensor matrix and on the other

hand, a tactile sensor matrix with two additional rotatory degrees of freedom (DOF). The planar tactile sensor module (DSA 9330/9335, [11]) used for both sensor versions is able to pick up a pressure profile using a resistive working principle. The second tactile sensor system actually consists of two sensors: a tactile sensor module which is mounted on an ultra-miniature joystick. The compliant mini-joystick (CTS Series 254, [12]) gives the tactile sensor module two additional rotational degrees of freedom. We call these joints *passive* as they can not be actively actuated.

Main components of the resistive tactile sensor are a common electrode and sensing electrodes which are arranged as a matrix. These electrodes are covered with conductive foam. The application of pressure on this sensor leads to an image of the applied pressure profile. As already investigated [13], the sensor's working principle depends on an interface effect between the metal electrodes and the structured sensor material, as pictured in Fig. 2(a). The resistance between the common (reference) electrode and a sensor cell electrode is a function of the applied load and time. Further details on the sensor's working principle can be found in [13]–[15].

The compliant mini-joystick consists of two potentiometers with each measuring a rotational angle of 50 degrees. The determined resistances can be associated with the current angles of the mini-joystick. Due to their resistive working principle, the potentiometers can be connected to the existing sensor controller used for the tactile sensor module. Fig. 2(b) illustrates how the mini-joystick is integrated into the existing tactile sensor modules whereas Fig. 2(c) shows a close-up of the new finger tip.

B. Sensor system of the anthropomorphic robot hand

To build our hand, we used an anthropomorphic robot hand [16] with eight degrees of freedom. The thumb, the index and the middle finger have 2DOF in each case. The ring and the tiny finger respectively have 1DOF at the proximal phalanx. The hand is actuated pneumatically with position control of the fingers. The electronic part of the robotic hand consists of fluidic actuators, joint angle sensors and a hand motion controller.

As introduced in [14], we developed a construction kit using tactile sensor modules, a sensor controller (DSACON32-M with modified firmware [11]), printed circuit boards carrying additional electronic components and the corresponding hardware to assemble all these parts into the robot hand.

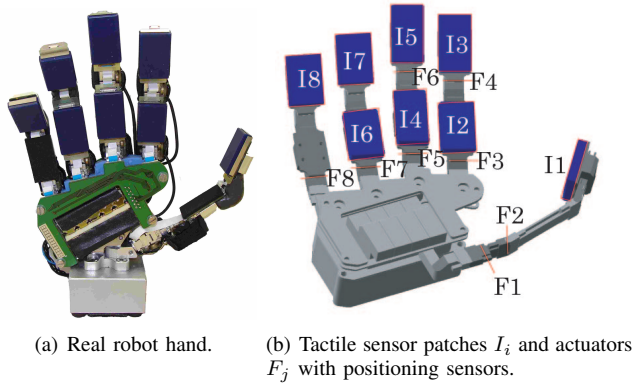


Fig. 3. Sensor layout of the anthropomorphic robot hand.

To cover the inner surface of the fingers, only two different sensor modules (with a different length but same width – resolutions of 4×7 and 4×6 taxels are available) are necessary. The index, the middle and the ring finger have 2 tactile sensor modules in each case. The thumb and the tiny respectively have only one single sensor module at the distal phalanx. Main parts of the electronic system are the tactile sensor modules, the tactile sensor controller, a communication subsystem and the existent hardware of the robotic hand. Fig. 3 shows the real robotic hand as well as the sensor and actor configuration of the robot hand.

The second version of the hand is additionally equipped with the enhanced version of the tactile sensor system using mini-joysticks. For this purpose, the existing construction kit can be completely reused without modification. The joystick modules need a supply voltage and provide two analog signals. The analog output signals are connected to a multiplexer which is connected again to the digital address bus and the A/D converter of the sensor controller. The 5 compliant finger tips make 10 additional passive degrees of freedom for the robot hand.

III. TACTILE SIGNAL PROCESSING

For feature extraction two approaches are considered in this work: a moment analysis for computing the position, area and eccentricity of a contact as well as a principal component analysis for finding a low-dimensional subspace for tactile contact patterns. The aim is a dimension reduction of the tactile patterns while keeping the essential information.

A. Moment Analysis

As the data of the tactile sensor matrix corresponds to a two-dimensional planar image, we analyze these images using moments up to the 2^{nd} order [17]. The two-dimensional $(p+q)^{th}$ order moment $m_{p,q}$ of an image is defined as the following double sum over all image pixels (x, y) and their values $f(x, y)$:

$$m_{p,q} = \sum_x \sum_y x^p y^q f(x, y) \quad p, q \geq 0 \quad (1)$$

The moment $m_{0,0}$ constitutes the total area of the object imprinted on the sensor. The centroid $\vec{x}_c = (x_c, y_c)^T$ of this

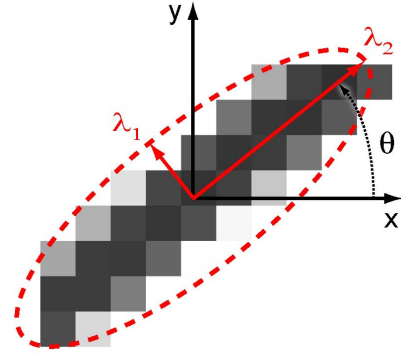


Fig. 4. Output of the moment analysis: the position (x, y) and the eigenvalues λ_1, λ_2 of a contact region. The orientation θ is not used.

area can be computed to

$$x_c = \frac{m_{1,0}}{m_{0,0}}, y_c = \frac{m_{0,1}}{m_{0,0}} \quad (2)$$

Furthermore, the centroid is needed to calculate the higher order moments, the so-called *central moments* $\mu_{p,q}$:

$$\mu_{p,q} = \sum_x \sum_y (x - x_c)^p (y - y_c)^q f(x, y) \quad p, q \geq 0 \quad (3)$$

The 2^{nd} order central moments can be used to compute the principal axes of the object which approximate the image by an ellipse.

The eccentricity ϵ of a contact is described by the relation of the eigenvalues λ_1 and λ_2 of the matrix $\begin{bmatrix} \mu_{2,0} & -\mu_{1,1} \\ -\mu_{1,1} & \mu_{0,2} \end{bmatrix}$. If both eigenvalues have a similar value, then the contact area tends to have a round or square shape and the eccentricity is close to zero.

Touching an edge results in an oblong ellipse with an eccentricity ϵ close to 1 when using

$$\epsilon = \frac{(\mu_{2,0} - \mu_{0,2})^2 + 4\mu_{1,1}^2}{(\mu_{2,0} + \mu_{0,2})^2} \quad \epsilon \in [0, 1] \quad (4)$$

Each tactile image I_i can then be described by the vector $(x, y, \epsilon, \lambda_1)$, as illustrated in Fig. 4. Alternatively, a binary presentation for each tactile image is considered: “having contact” or “having no contact”. A tactile sensor patch has contact, if $m_{00} > \delta$ with δ as a predefined pressure threshold.

B. Principal Component Analysis

A principal component analysis (PCA) is used for identifying the characteristic features of given contact pattern examples. For the PCA n tactile images are given. With \underline{I} as one of these images of the size $w \times h$, the vector representation is given by the vector \vec{v} of size $s = w \cdot h$.

$$\underline{I} = \begin{pmatrix} I_{11} & \cdots & I_{w1} \\ \vdots & \ddots & \vdots \\ I_{1h} & \cdots & I_{wh} \end{pmatrix}$$

$$\Rightarrow \vec{v} = (I_{11} \cdots I_{w1}, I_{12} \cdots I_{w2} \cdots I_{1h} \cdots I_{wh})^T$$

The mean vector is computed to

$$\bar{\mu} = \sum_{i=1}^n \frac{1}{n} \bar{v}_i. \quad (5)$$

The covariance matrix is given by

$$\underline{K} = \frac{1}{n} \sum_{i=1}^n (\bar{v}_i - \bar{\mu})(\bar{v}_i - \bar{\mu})^T \quad (6)$$

which is of size $s \times s$.

The principal component analysis of \underline{K} results in s eigenvalues Λ_i and the accordant eigenvectors γ_i , which span the orthogonal eigenspace $\Gamma = (\gamma_1, \dots, \gamma_p)$. This eigenspace describes the highest variance between the images. The $s \times s$ -matrix, with each eigenvector as a column, is reduced to a $s \times d$ -matrix \underline{E} by taking only the first d eigenvectors with highest eigenvalues. Given an image in vector presentation \bar{v} and the reduced eigenvector matrix \underline{E} the image vector is reduced to a $d \times 1$ -vector by $\bar{k} = \underline{E}^T \cdot \bar{v}$ which is used as the final presentation of a tactile image. Given a set of tactile images, these images are transferred into a vector representation. Then, a lower dimensional subspace is computed from the given examples by a principal component analysis. This subspace optimally represents the given contact patterns.

We consider two possibilities for applying the PCA: treat each tactile image independently gaining an input space of 4×7 taxels or group the two tactile images of each finger together gaining an input space of 8×7 taxels.

IV. IDENTIFYING HAPTIC KEY FEATURES

A. Grasping Strategy

In order to enfold an object with the robot hand and to acquire haptic data, a simple strategy for closing the hand is needed. In order to simplify the test scenario, the object is handed over to the robot by laying it into the opened robot hand. Therefore, the robot does not have to approach and grasp the object. Furthermore, the robot hand must adapt itself to the shape of the object in order to capture the variety of partial shapes of the object. As depicted in Fig. 5, the process of enfolding an object is done in two steps:

- 1) Only the proximal phalanges of the robot hand are closed. A movement of a finger is stopped if a contact is detected for this finger. A contact is detected if the desired finger movement deviates from the executed finger movement. After all finger movements have stopped, tactile imprints of all tactile sensor patches are taken.
- 2) The distal phalanges are closed as well until each finger has contact or reached the maximum angle. Again, tactile imprints of all tactile sensor patches are taken.

For a single palpation, we get $2 \cdot 8$ angles for the finger configuration and $2 \cdot 8$ tactile images. Using the new version of the hand, we gain 10 additional angles for the orientation of the tactile sensor planes of the finger tips.



Fig. 5. Enfolding an object: (1) The object is laid into the opened robot hand. (2) The proximal phalanges of the robot hand are closed. (3) Finally, the distal phalanges are closed as well.

B. Haptic key features

A single palpation is represented by a tuple (\vec{F}, \underline{I}) with \vec{F} as the kinesthetic data including the finger positions and \underline{I} as the tactile images. Applying the feature extraction from section III, the set of tactile images in \underline{I} is transferred to a set of tactile features \vec{I} . We want to use a limited set of haptic key features to describe a palpation sequence. Instead of using a manually predefined primitive set, we use a clustering method to identify which combination of finger configurations and contact patterns is most suitable to describe an object. For identifying haptic key features we apply a vector quantisation on the finger configurations and the contact patterns independently. The output of this clustering consists of f representative vectors for finger configurations and t for the contact patterns. The number of clusters has to be predetermined. For identifying haptic key features, we introduce the Self-Organizing Maps in the next chapter as a machine learning approach.

C. Self-Organizing Maps

A self-organizing map [18] (SOM) is described by a set of neurons. Each neuron c_i is assigned to a n-dim. weight vector m_i and a position r_i on the map. Each neuron represents a currently unknown category. During the training process each input pattern is assigned to one of these categories and simultaneously, the discrimination between the categories becomes more precisely with each step of the training. Thus, the training process of a SOM describes a structure-preservative mapping from high-dimensional input space to a 2-dim. output space. Similar patterns in the input space lie in a geographical near position in the output space. Of course, this mapping concurs with inaccuracy. As a benefit, the clustered high-dimensional input data can be simply visualized on a regular grid.

The training of a SOM is based on competitive learning: the idea is the adaptation of a neuron c with highest activation energy with respect to a randomly picked pattern x , so that in the future higher activation energy is achieved with the same input. Here, the activation energy complies with the Euclidean distance between the weight and the input vectors. The SOM can be referred to as an unsupervised learning or clustering method.

One training run t consists of 4 steps:

- 1) Pick a random input vector $x(t)$.
- 2) Calculate distance between weight vectors and input vector:

$$D_i(t) = \|x(t) - m_i(t)\|.$$

3) Determine winner neuron c :

$$c = \underset{i}{\operatorname{argmin}}(D_i(t)).$$

4) Adapt weight neurons in the neighborhood of the winner:

$$m_i(t+1) = m_i(t) + \alpha(t) \cdot h_{ci}(t) \cdot [x(t) - m_i(t)].$$

The neighborhood function is given by:

$$h_{ci}(t) = \exp \frac{\|r_c - r_i\|^2}{2 \cdot \sigma(t)^2}.$$

An adaptation means the movement of the weight vectors into the direction of the input vectors. The learning process determinates by reducing the learning rate $\alpha(t)$ and the neighborhood $h_{ci}(t)$. The SOM converges to a stable state, if no further changes occur.

The use of a $w \times h$ SOM results into $w \cdot h$ categories for describing an input pattern. After training, the SOM can be used for assigning a pattern to one of the determined classes by the function $S(x)$:

$$k = S(x) = \underset{i}{\operatorname{argmin}}(\|x - m_i\|) \in [1, w \cdot h] \quad (7)$$

In a vector representation, this can be written as a $n \cdot m$ zero vector with a value one at position k . We will use this vector representation in the following. A soft decision can be made by weighting each weight neuron by its distance to the input pattern.

V. OBJECT CLASSIFICATION WITH HAPTIC KEY FEATURES

A. Object descriptor

A palpation sequence consists of n single palpations (A_1, A_2, \dots, A_n) . A single palpation itself is represented by a tuple (\vec{F}, \vec{I}) with \vec{F} as the finger configuration and \vec{I} as the processed tactile images.

Due to the inhomogeneity of the tactile and the kinesthetic data, we apply a clustering for the sensor modalities independently. Then, a sequence of finger positions F_i can be described using the SOM-function S_f trained with finger positions:

$$(F_1, F_2, \dots, F_n) \Rightarrow (S_f(F_1), S_f(F_2), \dots, S_f(F_n))$$

As we do not consider the order of the palpations, the fusion of the palpation sequence of the length n is made by building a histogram of the key features. This simply results from the sum over the classification vectors of the whole palpation sequence:

$$\vec{O}_f = \sum_{i=1}^n S_f(F_i) \quad (8)$$

Then, each entry of the vector \vec{O}_f describes how often the corresponding finger configuration has been chosen to enfold an object.

To compare two palpation sequences with a different amount of palpations, we have to normalize the object vector with respect to the length of the sequence:

$$\vec{O}_f = \frac{1}{n} \vec{O}_f = \frac{1}{n} \sum_{i=1}^n S_f(F_i) \quad (9)$$

Now, each entry of the vector \vec{O}_f describes the percentage of how often the corresponding class was used to describe a palpation. We use this representation as a final object descriptor for classification. The same procedure is applied to tactile data gaining an object descriptor \vec{O}_t .

For classification we use a Bayes classifier explained in the following section. The classifier C generates a vector \vec{y} with an output dimension corresponding to the numbers of the objects to be classified. We propose two different approaches for the fusion of tactile and kinesthetic data:

- 1) **Description Fusion:** The object descriptors of the tactile and the kinesthetic data are concatenated into one description resulting into a classification $C(\vec{O}_f, \vec{O}_t)$. Having n clusters for the tactile data and m for the kinesthetic data, the vector size becomes $m + n$.
- 2) **Decision Fusion:** The classification is done with tactile and kinesthetic data independently. Afterwards, the classification results are merged into one decision: $w \cdot C_f(\vec{O}_f) + (1 - w) \cdot C_t(\vec{O}_t)$ with w as the weight for the two classifiers.

B. Bayes classifier

Statistical learning approaches for pattern recognition use statistical coherence in training data to create a classifier. The *Bayes rule* is of utmost importance as it allows to determine the probability of a certain reason for an observed effect. The observations are named D and possible reasons are called hypotheses h . Then, the Bayes rule is given by

$$P(h|D) = \frac{P(D|h)P(h)}{P(D)} \quad (10)$$

and is derived from the definition of the conditional probability. We are interested to find the hypothesis \hat{h} from a set of hypotheses $h \in H$, which maximize $P(h|D)$. In our case, h represents an object class and D an observed object descriptor. The term $P(D)$ can be left out as it does not influence the maximization. As we assume that all hypotheses have the same a-priori probability $P(h)$, the maximization results into the *Maximum-Likelihood-hypothesis*:

$$h_{\text{ML}} \equiv \underset{h \in H}{\operatorname{argmax}} P(h|D) = \underset{h \in H}{\operatorname{argmax}} P(D|h) \quad (11)$$

The probability $P(D|h)$ for each class is approximated by a multivariate normal distribution which is defined by the mean vector $\vec{\mu}$ and the covariance matrix Σ of the related training descriptors. Any pattern is assigned to the class with the most likelihood or by weighting the vote according to the probabilities.

VI. RESULTS

For the evaluation of this approach, a human being repeatedly hands over the unknown object to the robot hand. This corresponds to a palpation sequence where the robot repeatedly enfolds the object without knowing the exact object position. Fig. 6 shows the objects which were used for evaluation. The questions we want to investigate are:

- How good is the object recognition approach?
- How important are tactile and kinesthetic data?
- How to merge tactile and kinesthetic data?
- What is the relation between the recognition rate and the number of palpations?
- What is the improvement of the new tactile sensor type?

For the evaluation of our approach we used initially the first version of the hand with rigid tactile sensor modules. For the moment analysis, we used the features mean-x, mean-y, eccentricity and major axis length. These values were normalized between $[0, 1]$. For the PCA, we processed the images of the tactile sensors separately. Each image was upscaled by factor 2 gaining an input size for the PCA of 14×8 . The output dimension of the dimension reduction based on the PCA is 10. For the clustering, we used a 6×6 -SOM on finger positions and a 8×8 -SOM on image data. If not explicitly stated, decision fusion and 3 palpations for a sequence were used. We used for training 50 sequences for each object. This makes 150 palpations for an object class for training. Similarly, we recorded for each object 35 sequences for testing.

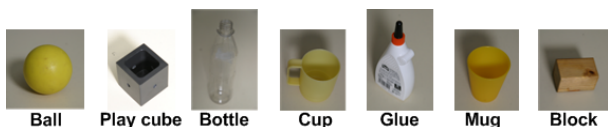


Fig. 6. The 7 Objects used for evaluation.

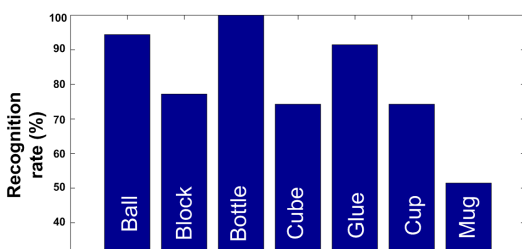


Fig. 7. Single Recognition Rates.

Fig. 7 shows the single recognition rates. The ball, the bottle and the glue were recognized over 90%. The wooden block, the play cube and the cup have still a recognition rate of over 74%. Surprisingly, the recognition rate of the mug is only close to 50%.

To find the best way of merging the two sensor modalities, we have a look at Fig. 8. We used a moment analysis for tactile feature extraction. Applying decision fusion, we used for summing up both decisions a weight of 0.5. The performance of object recognition with position and with

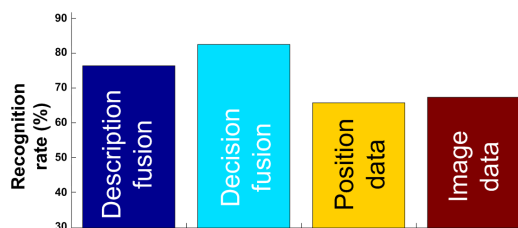


Fig. 8. Comparison of description fusion, decision fusion and recognition just based on a single sensor modality.

image data is almost equal. It becomes obvious that fusion of both modalities improves the results in general. So none of the two sensor modalities is more appropriate for object recognition although the finger positions were expected to achieve better results. By merging the decision vectors by a weighted sum, the best results were achieved.

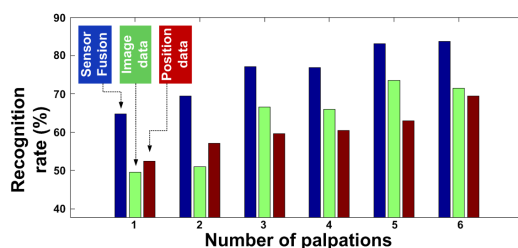


Fig. 9. The relation of recognition rate to the number of palpations - comparing sensor fusion, image data only and position data only.

Fig. 9 plots the relation between recognition rate and the number of palpations. We used an increasing number of palpations from 1 to 6. The recognition rate becomes in general better with an increasing number of palpations - this applies to both sensor modalities and to the fusion of them as well. This agrees with the idea of examining an entire sequence of palpations instead of just a single palpation. Furthermore, it shows that the fusion of a sequence works with a different number of palpations.

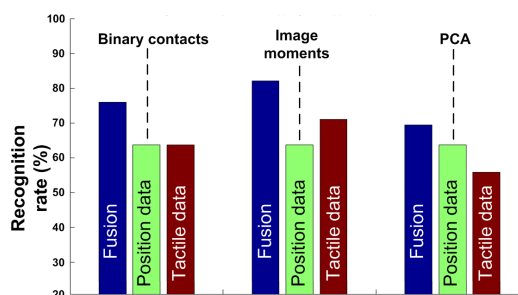


Fig. 10. Comparison of different tactile feature types: binary contacts, image moments and PCA.

For finding the best way for extracting features from tactile data, PCA, image moments and simple binary contacts were compared as depicted in Fig. 10. The tactile features based on moment analysis achieved in general the best results. This result encourages us to further investigate tactile feature extraction using a dense matrix of tactile sensors.

Finally, Fig. 11 shows the benefit of the new finger tip. The planar tactile sensor matrices passively adapt their orientation until the normal of the tactile sensor plane almost agrees with object surface normal. We consider the additional passive joints as kinesthetic data. This good impression is confirmed by the evaluation pictured in Fig. 12. It compares the recognition rate of single objects regarding the sensor type and only considering the kinesthetic data. All objects except the glue bottle were recognized much better – especially the ball and the block. The additional kinesthetic sensor data improves the performance of the haptic recognition.

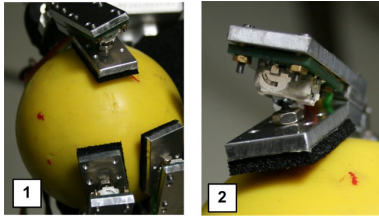


Fig. 11. The two rotatory degrees of freedom: (1) The finger tips of thumb, index and middle finger adapt themselves to the surface of the ball. (2) A close-up of the thumb.

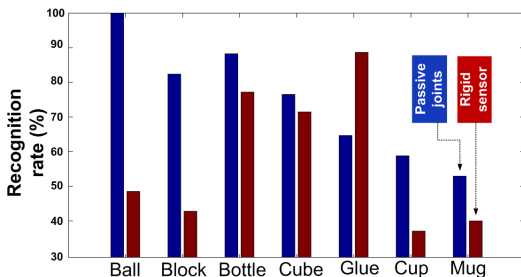


Fig. 12. Comparison of sensor versions – enhanced sensors with passive joints and standard rigid sensors: recognition rates based on kinesthetic data only.

VII. CONCLUSIONS AND FUTURE WORKS

This work introduced an approach which classifies an object directly from the finger positions and tactile patterns of an anthropomorphic robot hand. Using haptic key primitives as a compact description, a sequence of palpations can be merged into a simple statistical object description. This approach worked for most of the tested objects. The objects don't have to be fixed and are allowed to be moved. No hand kinematics must be known.

Furthermore, this paper introduced a versatile tactile sensing system consisting of a planar tactile sensor matrix mounted on a mini-joystick. The planar sensor surface adapts its orientation passively to the object surface and gathers additional information for perceiving the object shape. These additionally rotatory degrees of freedom improve the object recognition process.

For future work we will further investigate and improve the new finger tip – especially for grasping and exploration.

Furthermore, we will try to improve recognition rates and consider autonomous enfolding of objects. A focus will be on the improvement of the tactile signal processing, e.g. using extensions of the PCA.

VIII. ACKNOWLEDGMENTS

This work was supported by the German Research Foundation (DFG) within the Collaborative Research Center SFB 588 on “Humanoid robots—learning and cooperating multi-modal robots”.

REFERENCES

- [1] A. M. Okamura and M. R. Cutkosky, “Feature detection for haptic exploration with robotic fingers,” *Int. Journal of Robotic Research*, vol. 20, no. 12, pp. 925–938, 2001.
- [2] K. Weiss and H. Wörn, “Tactile sensor system for an anthropomorphic robotic hand,” in *Proc. of the IEEE/RAS Int. Conf. on Humanoid Robots, Santa Monica (CA), USA, 2004*.
- [3] P. A. Schmidt, E. Maël, and R. P. Würtz, “A sensor for dynamic tactile information with applications in human-robot interaction and object exploration,” *Robotics and Autonomous Systems*, vol. 54, no. 12, pp. 1005–1014, 2006.
- [4] P. Allen and K. Roberts, “Haptic object recognition using a multi-fingered dextrous hand,” in *Proc. of IEEE Int. Conf. on Robotics and Automation*, 1989, pp. 342–247.
- [5] C. Magnanini and F. Zanichelli, “Haptic object recognition with a dextrous hand based on volumetric shape representations,” in *Proc. of the IEEE Int. Conf. on Multisensor Fusion and Integration, Las Vegas, NV, 1994*, pp. 2–5.
- [6] G. Heidemann and M. Schoepfer, “Dynamic tactile sensing for object identification,” in *Proc. of the IEEE Int. Conf. on Robotics and Automation ICRA*, New Orleans, USA, 2004, pp. 813–818.
- [7] M. Johnsson, R. Pallbo, and C. Balkenius, “A Haptic System for the LUCS Haptic Hand I,” in *Mechanisms, Symbols, and Models Underlying Cognition: Int. Work-Conf. on the Interplay Between Natural and Artificial Computation, Las Palmas, Spain, 2005*, pp. 386–395.
- [8] M. Johnsson and C. Balkenius, “Experiments with proprioception in a self-organizing system for haptic perception,” in *Towards Autonomous Robotic Systems*, Aberystwyth, UK, 2007, pp. 239–245.
- [9] S. Takamuku, A. Fukuda, and K. Hosoda, “Repetitive grasping with anthropomorphic skin-covered hand enables robust haptic recognition,” in *Proc. of Int. Conf. on Intelligent Robot Systems, Nice, France, 2008*, pp. 3212–3217.
- [10] A. Schneider, J. Sturm, C. Stachniss, and W. B. Marc Reiser, Hans Burkhardt, “Object identification with tactile sensors using bag-of-features,” in *Proc. of the Int. Conf. on Intelligent Robot Systems, St. Louis, USA, 2009*.
- [11] Weiss Robotics, “Tactile sensor module, type: DSA 9335,” accessed 10/09/2009. [Online]. Available: <http://www.weiss-robotics.de/>
- [12] CTS Electrocomponents, “Series 254 Ultra-miniature Joystick,” accessed 10/09/2009. [Online]. Available: <http://www.ctscorp.com/>
- [13] K. Weiss and H. Wörn, “The working principle of resistive tactile sensor cells,” in *Proc. of the IEEE Int. Conf. on Mechatronics and Automation, Canada, 2005*.
- [14] D. Göger, N. Gorges, and H. Wörn, “Tactile Sensing for an Anthropomorphic Robotic Hand: Hardware and Signal Processing,” in *Proc. of the IEEE Int. Conf. on Robotics and Automation, May 12 - 17, 2009, Kobe, Japan, 2009*.
- [15] D. Göger and H. Wörn, “A highly versatile and robust tactile sensing system,” in *Proc. of the IEEE Conf. on Sensors, Atlanta (GA), USA, 2007*.
- [16] A. Schulz, C. Pylatiuk, A. Kargov, R. Oberle, and G. Bretthauer, “Progress in the development of anthropomorphic fluidic hands and their applications,” in *Mechatronics & Robotics 2004*, September 2004, pp. 936–941.
- [17] M.-K. Hu, “Visual Pattern Recognition by Moment Invariants,” *IEEE Transactions on Information Theory*, vol. 8, no. 2, pp. 179–187, 1962.
- [18] T. Kohonen, “Self-organized formation of topologically correct feature maps,” *Biological Cybernetics*, vol. 43, no. 1, pp. 59–69, January 1982.